A&A 471, 17–29 (2007)
DOI: 10.1051/0004-6361:20066478

Astronomy & Astrophysics

A study of catalogued nearby galaxy clusters in the SDSS-DR4

I. Cluster global properties⋆

J. A. L. Aguerri, R. Sánchez-Janssen, and C. Muñoz-Tuñón

Instituto de Astrofísica de Canarias C/ vía Láctea s/n, 38200 La Laguna, Spain
e-mail: [jalfonso;ruben;cmt]@iac.es

Received 29 September 2006 / Accepted 4 April 2007

ABSTRACT

Context. Large surveys such as the Sloan Digital Sky Survey have made large amounts of spectroscopic and photometric data of galaxies available, thereby providing important information for studying galaxy evolution in dense environments.
Aims. We have selected a sample of 88 nearby ($z < 0.1$) galaxy clusters from the SDSS-DR4 with redshift information for the cluster members. In particular, we focus on the galaxy morphological distribution, the velocity dispersion profiles, and the fraction of blue galaxies in clusters.
Methods. Cluster membership was determined using the available velocity information. We derived global properties for each cluster, such as their mean recessional velocity, velocity dispersion, and virial radii. Cluster galaxies were grouped into two families according to their $u - r$ colours.
Results. The total sample consists of 10 865 galaxies. As expected, the highest fraction of galaxies (62%) turned out to be early-type (red) ones, located at smaller distances from the cluster centre and showing lower velocity dispersions than late-type (blue) ones. The brightest cluster galaxies are located in the innermost regions and show the smallest velocity dispersions. Early-type galaxies also show constant velocity dispersion profiles inside the virial radius and a mild decline in the outermost regions. In contrast, late-type galaxies show ever decreasing velocity dispersions profiles. No correlation has been found between the fraction of blue galaxies and cluster global properties,such as cluster velocity dispersion or galaxy concentration. In contrast, we find a correlation between the X-ray luminosity and the fraction of blue galaxies.
Conclusions. These results indicate that early- and late-type galaxies may have had different evolutions. Thus, blue galaxies are located in more anisotropic and radial orbits than early-type ones. Their star formation seems to be independent of the cluster global properties in low-mass clusters, but not for the most massive ones. We consider that it is unlikely that the whole blue population consists of recent arrivals to the cluster. These observational results suggest that the global environment could be important for driving the evolution of galaxies in the most massive cluster ($\sigma > 800$ km s^{-1}). However, the local environment could play a key role in the galaxy evolution for low-mass clusters.

Key words. galaxies: clusters: general

1. Introduction

The large amount of spectroscopic and photometric data obtained during the past few years by surveys such as the Sloan Digital Sky Survey (SDSS; York et al. 2000) or the 2dF Galaxy Redshift Survey (2dFGRS; Colless et al. 2001) have opened a new horizon for studying galaxy evolution in particular, and studying galaxy clusters. It is well known that the environment plays an important role in the evolution of galaxies, and it is one of the key issues that a good galaxy evolution theory should address. There are several physical mechanisms, not present in the field, that can dramatically transform galaxies into high-density environments. Galaxies in clusters can evolve due to, e.g., dynamical friction, which can slow down the more massive galaxies, circularise their orbits, and enhance their merger rate (den Hartog & Katgert 1996; Mamon 1992). Interactions with other galaxies and with the cluster gravitational potential can disrupt the outermost regions of the galaxies and produce galaxy morphological transformations from late- to early-types (Moore et al. 1996), or even change massive galaxies into dwarf ones (Mastropietro et al. 2005). Swept of cold gas produced by ram-pressure stripping (Gunn & Gott 1972; Quilis et al. 2000) or swept of the hot gas reservoirs (Bekki et al. 2002) can alter the star formation rate (SFR) of galaxies in clusters. But it is still a matter of debate as to which of these mechanisms is the main one responsible for the galaxy evolution in galaxy clusters (see Goto 2005). Nevertheless, it is clear that all of these mechanisms transform galaxies from late- to early-types and can produce the different segregations observed in galaxy clusters.

One of the first segregations discovered in galaxy clusters was the morphological one. The first evidence of such a segregation date from Curtis (1918) and Hubble & Humason (1931), and was quantified by Oemler (1974) and Melnick & Sargent (1977). In his thorough work, Dressler (1980) analysed a sample of 55 nearby galaxy clusters, containing over 6000 galaxies, and observed that elliptical and S0 galaxies represent the largest fraction of galaxies located in the innermost and denser regions of galaxy clusters. In contrast, the outskirts of the clusters were dominated by spiral galaxies. In more distant clusters, the fraction of E galaxies is as large as or larger than in low-redshift clusters, but the S0 fraction is smaller (Dressler et al. 1997; Fasano et al. 2000). This has been interpreted as an evolution with redshift, where late-type galaxies are transformed into early-type ones. Segregations in velocity space have also been observed in galaxy clusters. Early observations found that

⋆ Table 1 is only available in electronic form at the CDS via anonymous ftp to cdsarc.u-strasbg.fr (130.79.128.5) or via http://cdsweb.u-strasbg.fr/cgi-bin/qcat?J/A+A/471/17

E and S0 galaxies showed smaller velocity dispersions than spirals and irregulars (Tammann 1972; Melnick & Sargent 1977; Moss & Dickens 1977). This has also been confirmed by other authors during the last two decades (Sodre et al. 1989; Biviano et al. 1992; Andreon et al. 1996; Stein 1997). The data from the ENACS survey (Katgert et al. 1998) produced a large sample of galaxies with spectroscopic redshifts and shed more light on this problem. Thus, Adami et al. (1998) studied a sample of 2000 galaxies, confirming early findings that the velocity dispersion of galaxies increases along the Hubble sequence: E/S0 galaxies show smaller velocity dispersions than early- and late-type spirals. This segregation was also observed in the velocity dispersion profiles (VDPs): late-type galaxies have decreasing VDPs, while E, S0, and early spirals show almost flat VDPs (Adami et al. 1998). The different kinematics shown by the different types of galaxies was analysed in more detail by Biviano & Katgert (2004), who found that the velocity segregation of the different Hubble types is due to differences in orbits. Thus, early-type spirals have isotropic orbits, while late-type ones are located on more anisotropic orbits. The observed morphological and velocity segregation in clusters have usually been used to conclude that late-type spiral galaxies in clusters are recent arrivals to the cluster potential (Stein 1997; Adami et al. 1998).

Star formation in galaxies is also affected by the environment. Butcher & Oemler (1984) found that the fraction of blue galaxies, f_b, in clusters is smaller than in the field and that it evolves with redshift: more distant clusters show higher values of f_b. This trend was interpreted as an evolutionary effect of the SFR in galaxy clusters. But the significant increase in new data has made it clear that the Butcher-Oemler effect is not only an evolutionary trend. A large scatter in the values of f_b has been observed in narrow redshift ranges (Smail et al. 1998; Margoniner & de Carvalho 2000; Goto et al. 2003), which suggests that the variation in f_b is influenced by environmental effects. In the past, many authors have tried to find correlations of f_b with cluster properties, such as X-ray luminosity (Andreon & Ettori 1999; Smail et al. 1998; Fairley et al. 2002), luminosity limit and clustercentric distance (Ellingson et al. 2001; Goto et al. 2003; De Propris et al. 2004), richness (Margoniner et al. 2001; De Propris et al. 2004), cluster concentration (Butcher & Oemler 1984; De Propris et al. 2004), presence of substructure (Metevier et al. 2000), or cluster velocity dispersion (De Propris et al. 2004). Some of these works have found correlations between f_b and the cluster environment while others did not, so that such a connection is still a matter of debate. However, these works were usually done using small and heterogeneous cluster samples (but see e.g., De Propris et al. 2004).

Environmental effects have also been invoked to explain the differences between the photometrical components of cluster and field spiral galaxies. Thus, it has been observed that the scale lengths of the disks of spiral galaxies in the Coma cluster are smaller than those of similar galaxies in the field (Gutiérrez et al. 2004; Aguerri et al. 2004). Interactions between galaxies or with the cluster potential can disrupt the disks of spiral galaxies in clusters. They can be strong enough for transforming bright late-type spiral galaxies in dwarfs (Aguerri et al. 2005a). The disrupted material would be part of the intracluster light already detected in some nearby galaxy clusters (Arnaboldi et al. 2002, 2004; Aguerri et al. 2005b) and galaxy groups (Castro-Rodríguez et al. 2003; Aguerri et al. 2006).

The observational results summarised before illustrate the important role played by environment in galaxy evolution. They also indicate that late-type and early-type galaxies in clusters are two different families of objects with different properties, which points to different origins or evolutions. Nevertheless, the main mechanisms responsible for this different evolution still remain unknown. In the present paper, we study one of the largest and more homogeneous galaxy cluster sample available in the literature. We have obtained the cluster membership, mean velocity, velocity dispersion, virial radius, and positions for a sample of 88 clusters located at $z < 0.1$. We investigated the main properties of a large sample of early (red) and late (blue) types of galaxies, such as their location within the cluster, their mean velocity dispersion, their VDPs, the $L_X - \sigma$ relation, and the fraction of blue galaxies for each cluster. This work provides important information about the properties of galaxies in nearby clusters, which will be useful for putting constraints on cosmological models of cluster formation. This is the first paper of a series in which we will analyse the properties of the dwarf galaxy population (Sánchez-Janssen et al., in preparation), substructure in galaxy clusters (Aguerri et al., in preparation), and composite luminosity function of galaxy clusters (Sánchez-Janssen et al., in preparation).

The paper is organised as follows. Section 2 shows the discussion about the galaxy cluster sample. The cluster membership and cluster global parameters are presented in Sect. 3. The results for the morphological segregation, velocity dispersion profiles, and the fraction of blue galaxies are given in Sects. 4–6, respectively. The discussion and conclusions are presented in Sects. 7 and 8, respectively. Throughout this work we have used the cosmological parameters: $H_0 = 75\,\mathrm{km\,s^{-1}\,Mpc^{-1}}$, $\Omega_m = 0.3$, and $\Omega_\Lambda = 0.7$.

2. Galaxy cluster sample

We have used photometric and spectroscopic data for objects classified as galaxies from the SDSS-DR4, an imaging and spectroscopic survey of a large area in the sky (York et al. 2000). The imaging survey was carried out through five broad-band filters, *ugriz*, spanning the range from 3000 to 10 000 Å, reaching a limiting r-band magnitude ≈22.2 with 95% completeness, and covering an area of 6670 deg^2 (Adelman-McCarthy et al. 2006). A series of pipelines process the imaging data and perfom the astrometric calibration (Pier et al. 2003), the photometric reduction (Lupton et al. 2002), and the photometric calibration (Hogg et al. 2001). Objects brighter than $m_r = 17.77$ were selected as possible targets for the spectroscopic survey, covering an area of 4783 deg^2 of the sky for the DR4. The spectroscopic data were obtained with optical fibers with a diameter of 3″ at the focal plane, resulting in a spectral covering in the wavelength range 3800–9200 Å with a resolution of $\lambda/\Delta\lambda \approx 2000$.

Our sample consists of all clusters with known redshift at $z < 0.1$ from the catalogues of Abell et al. (1989), Zwicky et al. (1961), Böhringer et al. (2000), and Voges et al. (1999), which have been mapped by the SDSS-DR4. We downloaded only those galaxies located within a radius of 4.5 Mpc around the centres of the galaxy clusters. Only those clusters with more than 30 galaxies with spectroscopic data in the searching radius were considered, resulting in a sample formed by 240 clusters following the previous criteria. The SDSS-DR4 spectroscopic galaxy target selection was done by an automatic algorithm (see Strauss et al. 2002). The main galaxy sample consists of galaxies with r-band Petrosian magnitudes brighter than 17.77 and r-band Petrosian half-light surface brightness brighter than 24.5 mag arcsec^{-2}. The completeness of this sample is high, exceeding 99% (see Strauss et al. 2002). However, some of the

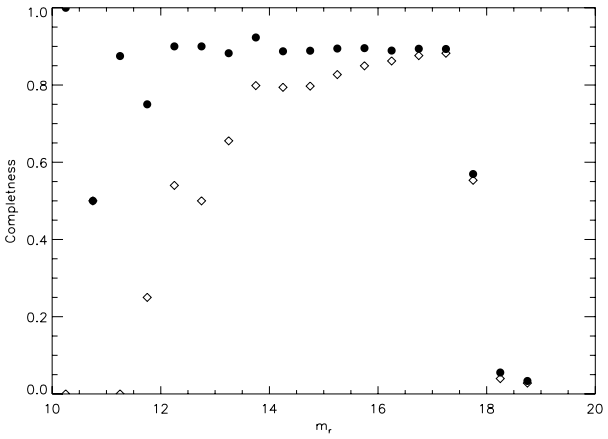

Fig. 1. Mean completeness of the cluster sample as a function of the r-band magnitude. Diamonds represent the spectroscopic data from SDSS-DR4 and black circles data after completion with data from NED.

selected spectroscopic targets were not observed at the end. This incompleteness has several causes, including that two spectroscopic fibers cannot be placed closer than 55″ on a given plate, possible gaps between the plates, fibers that fall out of their holes, and so on. For these reasons, we expect that the incompleteness of the spectroscopic data will be greater for bright galaxies in high-density environments such as galaxy clusters. Figure 1 shows the mean completeness[1] of the SDSS-DR4 spectroscopic data as a function of the r-band magnitude for the selected galaxies, where a fast increment towards faint magnitudes can be observed. In order to avoid possible effects on the results due to this effect, we completed the spectroscopic SDSS-DR4 observations with the data available at the Nasa Extragalactic Database (NED). Figure 1 also shows the mean completeness as a function of r-band magnitude after the spectroscopic data from NED were included in the sample. Notice that the new mean completeness is almost constant (≈85%) for all magnitudes brighter than $m_r = 17.77$. We made a second selection of the clusters by considering only those from our original list with completeness larger than 70% for galaxies brighter than 17.77 in the r-band.

3. Cluster membership

Clusters properties such as the mean cluster velocity, the velocity dispersion, the cluster centre, or the virial radius can be significantly affected by projection effects. Several methods have been developed during decades in order to obtain reliable galaxy cluster membership and avoid the presence of interlopers. They can be classified in two families: (i) those algorithms that use only the information in the velocity space, e.g. 3σ-clipping techniques (Yahil & Vidal 1977), gapping procedures (Beers et al. 1990; Zabludoff et al. 1990, hereafter ZHG algorithm), or the KMM algorithm (Ashman et al. 1994); (ii) those algorithms that use information on both position and velocity, such as the methods designed by Fadda et al. (1996), den Hartog & Katgert (1996), or Rines et al. (2003).

The cluster membership in our sample was obtained using a combination of two algorithms. A first rough cluster membership determination was obtained using the ZHG algorithm, which in a second step was then refined using the KMM algorithm. The ZHG algorithm is a typical gapping procedure that determines the cluster membership by the exclusion of those galaxies located at more than a certain velocity distance (Δv) from the nearest galaxy in the velocity space. Then, the mean velocity ($v_{\rm m}$) and velocity dispersion (σ) of the remaining galaxies are calculated. After sorting objects with velocities higher than $v_{\rm m}$, any galaxy separated in velocity more than σ from the previous one is classified as a non member. The same is done for those galaxies with velocities lower than $v_{\rm m}$. The process is repeated several times untill the mean cluster velocity ($v_{\rm c}$) and the cluster velocity dispersion ($\sigma_{\rm c}$) are finally obtained. Zabludoff et al. (1990) has pointed out that this method lacks statistical rigour and tends to give overestimated values for $\sigma_{\rm c}$. One of the disadvantages of this method is that the results obtained strongly depend on the chosen value of Δv. High values of Δv imply that a large fraction of interlopers are identified as cluster members. In contrast, low values of Δv result in the loss of cluster galaxies. We investigated the variation in $\sigma_{\rm c}$ for different values of Δv, finding that $\Delta v = 500$ km s^{-1} is an appropriate value for our clusters. This method also has the advantage that of easy implementation and it does not require too much computational time. Recently, it has been used in works involving a large number of clusters, such as those from the 2dFGRS (De Propris et al. 2003). The ZHG algorithm splits the velocity histograms into different galaxy groups, one of them located at the catalogued redshift of the cluster. That group was taken and analysed in more detail with the KMM algorithm. In the few cases where there was no galaxy group located at the catalogued redshift, we identified the most significant groups with $z < 0.1$ as the cluster itself.

The KMM algorithm (Ashman et al. 1994) estimates the statistical significance of bi-modality in a dataset. We have run it to the group of galaxies given by the ZHG algorithm, which contains the catalogued redshift of the cluster. The KMM algorithm gives us the compatibility of the velocity distribution of such group of galaxies with a single or multiple Gaussian distribution. We considered three different cases that are summarised in Fig. 2:

- Single cluster: the velocity distribution of the galaxies is compatible with a single Gaussian, e.g. Abell 757.
- Cluster with substructure: the velocity distribution is compatible with multiple groups. We identified the cluster as the group with the largest number of galaxies plus those groups that mean velocities lie within 3σ from the mean velocity of the largest one[2], e.g. Abell 1003.
- Cluster with contamination: the velocity distribution is compatible with the presence of several groups, but the mean velocities of the smaller groups deviate more than 3σ from the most populated one, which we identify as the cluster itself, e.g. Abell 168.

We have explored the differences in the values of $v_{\rm c}$ and $\sigma_{\rm c}$ if we consider as interlopers those groups of galaxies located at a velocity distance larger than 1σ or 3σ from the mean velocity of the main galaxy group. We find that the differences in $v_{\rm c}$ and $\sigma_{\rm c}$ in 90% of the clusters are less than 20%. The remaining 10% of the clusters are those with a significant structure in the velocity distribution, being most of them more than one cluster along the line of sight. Thus, we have adopted 3σ as the default except for those clusters with significant differences between 1σ and 3σ,

[1] We have defined the spectroscopic completeness per magnitude bin as the ratio of the number of galaxies with spectroscopic data to the number of galaxies with photometric information.

[2] In this case σ is the velocity dispersion of the largest group of galaxies.

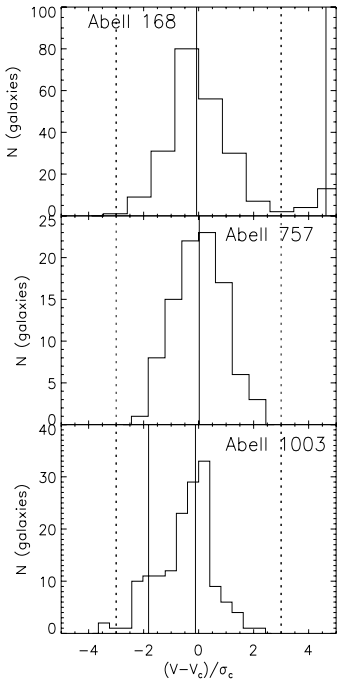

Fig. 2. Velocity histograms of three representative clusters of the sample. The vertical full lines represent the mean velocity of the different groups of galaxies in which KMM algorithm has divided the velocity histogram. The dotted vertical lines represent $v_c \pm 3\sigma_c$.

for which we measured the mean velocity and velocity dispersion of the cluster adopting the criteria of 1σ. Through all of this process, v_c and σ_c were determined using the biweight robust estimator of Beers et al. (1990).

3.1. Cluster global parameters

Once the cluster membership was determined, we obtained the global parameters of each cluster, i.e., mean velocity (v_c), velocity dispersion (σ_c), cluster centre, and the radius r_{200}. All of these parameters were computed using only the cluster members.

The determination of the cluster centre is important for accurately computing the other parameters of the clusters. The centre of the cluster is determined by the potential well, which can be traced by the position of the peak of the X-ray luminosity of the cluster. That peak was considered as the centre of those clusters from our sample with X-ray measurements in the literature. Unfortunately, not all the clusters from the sample have X-ray data. In that case, the centre of these clusters was determined by the peak of the galaxy surface density[3]. For those clusters with X-ray data, we compared the centres given by the peaks of X-ray luminosity and galaxy surface density, obtaining a mean difference of 150 kpc.

Analytic models (Gott 1972) and simulations (Cole & Lacey 1996) indicate that the virialized mass of clusters is generally contained inside the surface where the mean inner density is $200\rho_c$, where ρ_c is the critical density of the Universe. The radius of that surface is called r_{200}. We have computed the r_{200} for our clusters using the same approximation as Carlberg et al. (1997):

$$r_{200} = \frac{\sqrt{3}\sigma_c}{10\,H(z_c)}, \tag{1}$$

where $H(z_c)$ is the Hubble constant at the cluster redshift z_c.

The previous global parameters of the clusters (v_c, σ_c, r_{200}, and centre) were obtained as described above but in a recurrent way. In a first step, they were determined using all cluster member galaxies around 4.5 Mpc from the centre of the cluster. After this step we recalculated the parameters using only those galaxies located inside r_{200}. This method was repeated several times until the difference in the parameters obtained in two consecutive steps was less than 5%. Three or four iterations were usually enough for reaching the convergence. To obtain reliable parameters of the clusters, those with less than 15 galaxies within r_{200} were removed from our list. This results in a final sample formed by 110 nearby galaxy clusters. Table 1 shows the sample of galaxy clusters and their global parameters. The columns of Table 1 represent: (1) galaxy cluster name, (2, 3) cluster centres (α (J2000), δ (J2000)), (4) mean radial velocity, (5) cluster velocity dispersion, (6) r_{200} radius, (7) number of galaxies within r_{200}, and (8) spectroscopic completeness.

For 6 clusters (Abell 1003, Abell 1032, Abell 1459, Abell 2023, Abell 2241, and ZwCl1316.4-0044), large differences in the mean recessional velocity have been found between the values given in Table 1 and those from NED. These are the clusters with no significant galaxy group at the catalogued redshift (see Sect. 3).

To consider the possible influence of neighbouring clusters on the global properties of the sample, we searched in the surroundings of each cluster for the presence of companions. Following Biviano & Girardi (2003), we considered that two clusters, i and j, are in interaction when

$$|v_i - v_j| < 3(\sigma_i + \sigma_j) \qquad R_{i,j} < 2(r_{200,i} + r_{200,j}), \tag{2}$$

where $R_{i,j}$ is the projected distance between the centres of the clusters, and $v_{i,j}$, $\sigma_{i,j}$, $r_{200,i,j}$ their respective mean velocities, velocity dispersions, and r_{200}. We found 16 couples of clusters in interaction according to the previous criteria. The remaining sample (88 clusters) followed the isolation criteria and will be used in the analysis presented in the following sections. Figure 3 shows the sky distribution of the cluster members and the galaxy velocities as a function of clustercentric distance for a sample of 8 clusters, including the galaxies taken as cluster members and the interlopers. Notice the large number of interlopers in some of the galaxy clusters, such as Abell 1291, Abell 1383, Abell 2244. Some of them, Abell 1291 and Abell 1383, were not included in the final isolated sample due to the presence of companions.

3.2. Corrections to line-of-sight velocities

Line-of-sight velocities of galaxies in clusters were corrected by two effects: cosmological redshift and global velocity field. We should take into account that we are comparing the velocity dispersion of clusters located at different redshifts. Thus, for each galaxy we have $1 + z_{obs} = (1 + z_c)(1 + z_{gal})$ (Danese et al. 1980), with z_{obs} the apparent redshift of the galaxies, z_c the cosmological redshift of the cluster, and z_{gal} the redshift of the galaxy respect to the cluster centre. This correction can affect up to 10% of the most distant clusters in our sample.

Galaxy clusters are frequently part of larger cosmological structures such as filaments, superclusters, or multiple systems,

[3] The galaxy surface density was computed using the algorithm designed by Pisani (1996).

Table 2. Main properties of the different types of galaxies.

Galaxies within $r/r_{200} < 5$	$\langle r/r_{200}\rangle$	$\langle M_r\rangle$	$\langle\sigma\rangle$	$\langle\log(\Sigma)\rangle$	$N_{\rm gal}$
$u-r<2.22$	1.85 ± 0.02	-19.65 ± 0.01	1.04 ± 0.01	0.46 ± 0.08	4937
$u-r<2.22$ & $M_r<M_r^*-1$	1.79 ± 0.11	-21.54 ± 0.02	1.08 ± 0.09	0.40 ± 0.25	94
$u-r<2.22$ & $M_r^*-1<M_r<M_r^*+1$	1.90 ± 0.02	-20.00 ± 0.01	1.03 ± 0.01	0.38 ± 0.08	3126
$u-r<2.22$ & $M_r>M_r^*+1$	1.74 ± 0.03	-18.74 ± 0.02	1.05 ± 0.02	0.64 ± 0.14	1717
$u-r\geq2.22$	1.03 ± 0.01	-20.16 ± 0.01	0.90 ± 0.01	0.80 ± 0.05	5928
$u-r\geq2.22$ & $M_r<M_r^*-1$	0.95 ± 0.05	-21.62 ± 0.02	0.78 ± 0.03	0.89 ± 0.14	537
$u-r\geq2.22$ & $M_r^*-1<M_r<M_r^*+1$	1.10 ± 0.02	-20.20 ± 0.01	0.91 ± 0.01	0.75 ± 0.06	4592
$u-r\geq2.22$ & $M_r>M_r^*+1$	0.85 ± 0.04	-18.91 ± 0.02	0.90 ± 0.03	1.06 ± 0.12	729
Galaxies within $r/r_{200} < 2$	$\langle r/r_{200}\rangle$	$\langle M_r\rangle$	$\langle\sigma\rangle$	$\langle\log(\Sigma)\rangle$	$N_{\rm gal}$
$u-r<2.22$	0.97 ± 0.01	-19.61 ± 0.02	1.08 ± 0.02	0.80 ± 0.07	2636
$u-r<2.22$ & $M_r<M_r^*-1$	1.15 ± 0.07	-21.56 ± 0.03	1.18 ± 0.13	0.62 ± 0.24	54
$u-r<2.22$ & $M_r^*-1<M_r<M_r^*+1$	1.04 ± 0.01	-19.96 ± 0.01	1.08 ± 0.02	0.70 ± 0.07	1648
$u-r<2.22$ & $M_r>M_r^*+1$	0.85 ± 0.01	-18.70 ± 0.02	1.07 ± 0.03	1.02 ± 0.09	934
$u-r\geq2.22$	0.67 ± 0.01	-20.14 ± 0.01	0.91 ± 0.01	0.98 ± 0.04	4244
$u-r\geq2.22$ & $M_r<M_r^*-1$	0.57 ± 0.03	-21.65 ± 0.02	0.80 ± 0.03	1.02 ± 0.13	397
$u-r\geq2.22$ & $M_r^*-1<M_r<M_r^*+1$	0.69 ± 0.01	-20.19 ± 0.01	0.92 ± 0.01	0.94 ± 0.05	3239
$u-r\geq2.22$ & $M_r>M_r^*+1$	0.61 ± 0.02	-18.92 ± 0.02	0.89 ± 0.03	1.19 ± 0.10	608

which can affect the velocity field resulting in a modified cluster velocity dispersion. The interaction between galaxy clusters can also produce distorted velocity fields. We investigated the importance of these effects in the velocity field of our clusters by making a least-square fit to the radial velocities of cluster galaxies with respect to their position in the plane of the sky (see den Hartog & Katgert 1996; Girardi et al. 1996). For each fit we computed the coefficient of multiple determination, R^2. To test the significance of the fitted velocity gradients, we ran 1000 Monte Carlo simulations for each cluster for which the correlation between position and velocity was removed. This was achieved by shuffling the velocities of the galaxies with respect to their positions. We defined the significance of velocity gradients as the fraction of Monte Carlo simulations with R^2 smaller than the observed one. This correction of the velocity field was applied to those clusters in which the significance of velocity gradients is larger than 99% (30% of the total sample). However, this correction has small effects both in the shape of the velocity dispersion profiles and on the total velocity dispersion (the mean absolute correction was about 40 ± 15 km s^{-1}). This agrees with similar corrections applied in other cluster samples (den Hartog & Katgert 1996; Girardi et al. 1996).

3.3. Comparison with other methods

Some of the clusters presented in our sample have been previously studied by other authors. However, we have avoided comparing our results with those from the literature, given the different datasets used. To compare our cluster membership method with others proposed in the literature, we computed $\sigma_{\rm c}$ of our clusters with two more methods: a 3σ-clipping and the method proposed by Fadda et al. (1996). The median absolute difference between our $\sigma_{\rm c}$ and those computed by the 3σ-clipping method is only 17 km s^{-1}. Only 10% of the clusters show significant diferences ($\Delta\sigma_{\rm c} > 200$ km s^{-1}) in the computation of the velocity dispersion of the cluster with the two methods. They correspond to those clusters affected by a large amount of structure along the line of sight. The 3σ-clipping method gives considerably higher values of $\sigma_{\rm c}$ than ours for these clusters. Differences were larger when we compared ours with Fadda's method. In this case the mean absolute difference in $\sigma_{\rm c}$ between the two methods was 84 km s^{-1}, and 80% of the clusters show differences smaller than 200 km s^{-1}.

Recently, Popesso et al. (2006) have obtained the values of $\sigma_{\rm c}$ for a sample of Abell clusters using SDSS-DR4 data, for which cluster membership was obtained using the selection algorithm of Katgert et al. (2004). The median absolute difference between our and their $\sigma_{\rm c}$ is 45 km s^{-1} for the 28 clusters in common. Only for 4 clusters (Abell 1750, Abell 1773, Abell 2244 and Abell 2255) have the absolute differences in $\sigma_{\rm c}$ larger than 200 km s^{-1}.

We also compared our results with those given in the cluster catalogue presented by Miller et al. (2005). We found 16 clusters in common, with 74 km s^{-1} the median absolute difference between our and their $\sigma_{\rm c}$. In this case, 3 clusters show an absolute difference in $\sigma_{\rm c}$ larger than 200 km s^{-1}.

We can conclude that, in most of the cases, our cluster membership method reports values of $\sigma_{\rm c}$ similar to those given by other methods. Only for 10–20% of the clusters have the absolute differences in $\sigma_{\rm c}$ between our method and the others larger than 200 km s^{-1}. For these clusters the structure along the line of sight is responsible for the difference, with our $\sigma_{\rm c}$ values lower than the others.

3.4. $L_{\rm x}$–σ relation

We can learn about the nature of cluster assembly by studying the relations between cluster observables. One of the most universals is the well-known relation between the cluster X-ray luminosity and the velocity dispersion of its galaxies ($L_{\rm X}\propto\sigma_{\rm c}^b$). Cluster formation models predict that if the only energy source in the cluster comes from the gravitational collapse, then $b\approx4$. This relation has been studied in the literature by many authors using different cluster samples, finding values of b between 2.9 and 5.3 (Edge & Stewart 1991; Quintana & Melnick 1982; Mulchaey & Zabludoff 1998; Mahdavi & Geller 2001; Girardi & Mezzetti 2001; Borgani et al. 1999; Xue & Wu 2000; Ortiz-Gil et al. 2004; Hilton et al. 2005). The study of the $L_{\rm X}-\sigma_{\rm c}$ relation in our cluster sample will also be useful as another check for the values of $\sigma_{\rm c}$ we have derived. We have X-ray data for 48 galaxy clusters from our sample. The X-ray data were obtained from Ebeling et al. (1998, 2000), Böhringer et al. (2000), and Ledlow et al. (2003), and the X-ray luminosities are measured in the ROSAT band (0.1–2.4 keV).

Figure 4 shows the $L_{\rm X}-\sigma$ relation for this subset with available X-ray data in the literature. The Spearman coefficient of

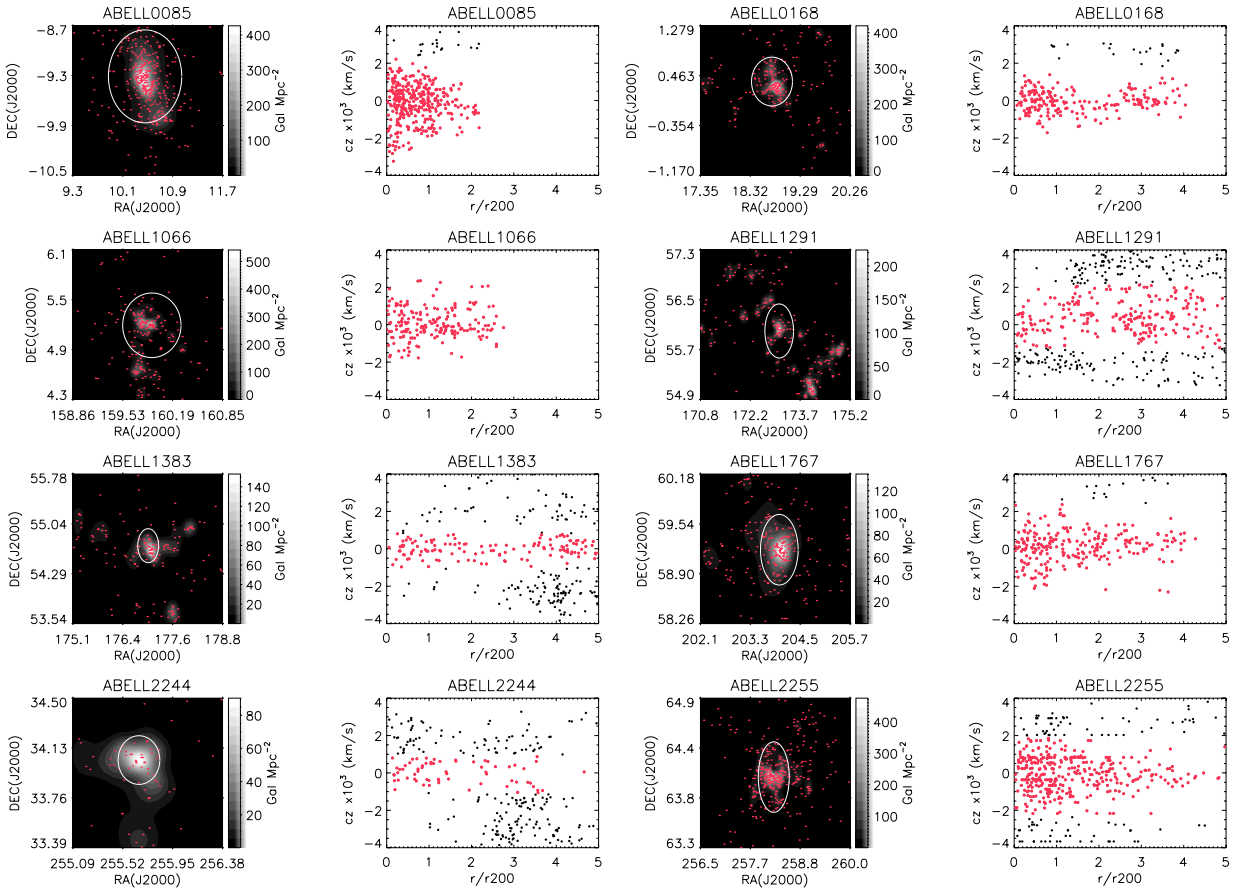

Fig. 3. Galaxy surface density (images) and radial velocity versus distance to the cluster centre for the galaxy cluster member (red points) of a subsample of 8 clusters. The overplotted circle have a radius equal to r_{200} for each cluster. The black points represent interloper galaxies.

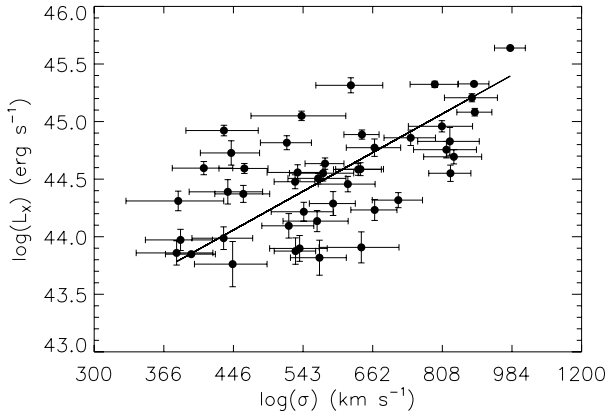

Fig. 4. $L_X - \sigma$ relation for the 48 galaxy clusters with X-ray data in the ROSAT band (0.1–2.4 keV) from our sample. The full line represents the best fit using the BCES bisector algorithm (see text for more details).

the relation is 0.56 and the significance from zero correlation is greater than 3σ. This indicates the existence of a correlation between L_X and σ_c for the clusters of our sample. We used the bivariate correlated errors and intrinsic scatter (BCES) bisector method of Akritas & Bershady (1996) to obtain the coefficient and power-law slope estimates of the relation. This fitting technique takes into account errors in both variables and intrinsic scatter. The $L_X - \sigma_c$ relation for our clusters is given by

$$L_X(0.1{-}2.4\,\mathrm{keV}) = 10^{33.7\pm1.2}\sigma^{3.9\pm0.4}. \quad (3)$$

This result is in very good agreement with another measurement of this relation using the same ROSAT band (0.1–2.4 keV) for the X-ray data and the same fitting algorithm (see Hilton et al. 2005).

3.5. Redshift distribution and sample completeness

The 88 isolated galaxy clusters are located in a redshift range between 0.02 and 0.1, with an average redshift of 0.071. Figure 5 shows the absolute r-band magnitude (M_r) as a function of the redshift for the galaxies in our cluster sample[4]. It is clear that the completeness magnitude is a function of redshift. This figure shows that the full sample is complete for galaxies brighter than $M_r = -20.0$. The lack of completeness for fainter galaxies will be taken into account in the subsequent analysis.

4. Morphological segregation

Light concentration or colours have been used extensively in the literature to classify galaxies. Shimasaku et al. (2001) and Strateva et al. (2001), using SDSS data, find that the ratio of Petrosian 50 percent light radius to Petrosian 90 percent light radius, C_{in}, measured in the r-band image was a useful index for quantifying galaxy morphology. Strateva et al. (2001) also find that the colour $u - r = -2.22$ efficiently separates early- and late-type galaxies at $z < 0.4$. We used colours for

[4] See Sect. 4 for the explanation of the computation of the absolute magnitudes of the galaxies.

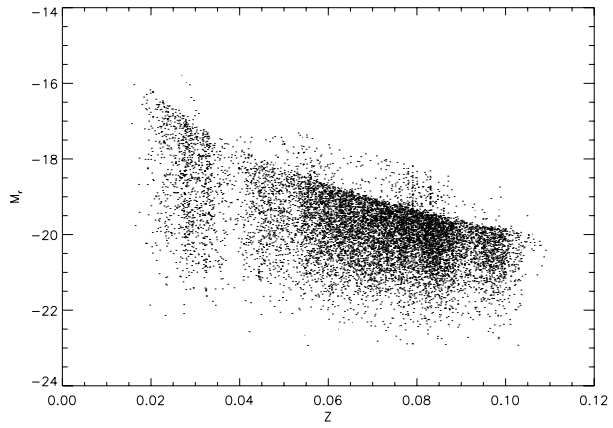

Fig. 5. Absolute r-band magnitude as a function of redshift for the galaxies of our cluster sample.

classifying galaxies, because properties such as velocity dispersion in galaxy clusters are better correlated with galaxy colours than is the galaxy morphology (Goto 2005). The magnitudes of the galaxies were corrected by two effects: Galactic absorption and k-correction. The Galactic absorption in the different filters was obtained from the dust maps of Schlegel et al. (1998). We applied the k-correction using the kcorrect.v4_1_4 code by Blanton et al. (2003) to obtain the rest-frame magnitudes of the galaxies for the different bandpasses. Once these two corrections were made, we classified the galaxies in red ($u - r \geq 2.22$) and blue ones ($u - r < 2.22$).

The galaxy data was downloaded from the SDSS database according to a metric criteria: we downloaded the information of all galaxies located within a radius of 4.5 Mpc at each galaxy cluster redshift. This means that we are mapping different physical regions for each cluster. To avoid this problem we studied the ratio $r_{\rm max}/r_{200}$ for each cluster, with $r_{\rm max}$ the maximum distance of a galaxy from the cluster centre for each galaxy cluster. We found that all clusters of our sample reach $\frac{r_{\rm max}}{r_{200}} = 2$, and 50% of them reach $\frac{r_{\rm max}}{r_{200}} = 5$.

Our sample of galaxies consists of 6880 galaxies located within a radius $2 \times r_{200}$, with 62% of them red galaxies and 38% blue ones. If we consider all galaxies within $5 \times r_{200}$, then the sample has 10865 galaxies, with 55% and 45% red and blue galaxies, respectively. The red and blue galaxies were also grouped in three categories according to their r-band magnitude: $M_r < M_r^* - 1$, $M_r^* - 1 < M_r < M_r^* + 1$, and $M_r > M_r^* + 1$[5]. The first group contains the brightest members of the clusters, the third group contains the so-called dwarf population and the second one is formed by normal bright galaxies. Table 2 shows the median location, r-band absolute magnitude, velocity dispersion, and local density[6] of the different galaxy groups. In general, red galaxies are brighter than blue ones and are also located closer to the cluster centre in higher local density regions. The two families of galaxies present different kinematics, in the sense that red galaxies show a smaller velocity dispersion than blue ones. This different kinematic between red and blue galaxies has also been seen in other studies and has been interpreted as red and blue galaxies having different kinds of orbits, where the orbits of blue galaxies are more anisotropic than the red ones (Adami et al. 1998; Biviano & Katgert 2004). Other authors interpret this difference in velocity dispersion as evidence that ram pressure is not playing an important role in the galaxy evolution of clusters. In contrast, tidal interactions should be the dominant mechanism (Goto 2005). All of these properties are independent of the sampled area.

It is also interesting that red dwarf galaxies are located in similar environments as the brightest red ones: close to the cluster centre in high local density regions (see also Hogg et al. 2004). But the red dwarf population shows a larger velocity dispersion than the brightest red galaxies. Biviano & Katgert (2004) find that the brightest cluster members are not in equilibrium with the cluster potential. They are special galaxies that could have formed close to the cluster centre or have fallen into this region due to dynamical friction. In contrast, dynamical friction is not very efficient in the dwarf population, so that the main presence of these galaxies in the central regions of the clusters should be due to their origin. The discussion about the properties and the origin of the dwarf population will be given in another paper (Sánchez-Janssen et al., in preparation).

5. Velocity dispersion profiles

The adopted cluster velocity dispersion was calculated with the galaxies located within the r_{200} radius of each cluster. How σ depend on the clustercentric distance in our sample can be answered by studying the integrated velocity dispersion profiles (VDPs) of the clusters. These profiles also provide information about the dynamical properties of the galaxies. Thus, a system with galaxies predominantly in radial orbits produces an outwardly declining VDP, while the opposite behaviour instead suggests that the galactic orbits are largely circular. In contrast, constant VDPs are characteristic of an isotropic distribution of velocities (Solanes et al. 2001). Figure 6 shows the VDPs for some of the clusters in our sample. They show the velocity dispersion of the cluster at a given radius evaluated using all the galaxies within that radius, without any restriction on their luminosities. The errors shown in Fig. 6 were computed using the approximation given by Danese et al. (1980).

To classify the VDPs of our clusters, we computed the velocity dispersion ($\sigma_i, i = 1, 2, 3, 4, 5$) of the galaxies in the clusters located within five different radii: $0.4 \times r_{200}$, $0.6 \times r_{200}$, $2 \times r_{200}$, $3 \times r_{200}$, and $4 \times r_{200}$, respectively. We compared these values with $\sigma_{\rm c}$, given in Table 1. The resulting mean ratios $\sigma_i/\sigma_{\rm c}$ were: 1.02 ± 0.04, 1.01 ± 0.01, 0.97 ± 0.01, 0.94 ± 0.02, and 0.94 ± 0.02, for $i = 1, 2, 3, 4, 5$, respectively. These values indicate that, within r_{200}, the VDPs of the total galaxy cluster population are consistent with being flat. The mean variation of the VDPs inside r_{200} is only 2%. The values of $\sigma_i/\sigma_{\rm c}, i = 3, 4, 5$ show that, outside r_{200}, the VDPs slowly decrease. The mean variation in the VDPs outside r_{200} is -6%. No differences in the ratios $\sigma_i/\sigma_{\rm c}$ have been found when we divided the galaxy sample between bright ($M_r < M_r^* + 1$) and dwarf ($M_r > M_r^* + 1$) galaxies. This flat behaviour of the VDPs inside r_{200} suggests that galaxies in these areas have an isotropic distribution of velocities. In contrast, the decline with the radius of VDPs outside r_{200} points to radial orbits (Solanes et al. 2001).

Figure 6 also shows the VDPs of early- (red) and late-type (blue) galaxies. In most profiles, the velocity dispersion of blue galaxies is larger than the corresponding one for early-type ones. We also analysed the shape of VDPs of blue and red galaxies, as we did for the total sample. For red galaxies, we found that $\sigma_i/\sigma_{{\rm c},r}$ are 1.04 ± 0.03, 1.03 ± 0.03, 0.97 ± 0.02, 0.96 ± 0.02, and 0.96 ± 0.03, for $i = 1, 2, 3, 4, 5$, respectively. The values

[5] $M_r^* - 5\log(h) = -20.04$, Blanton et al. (2005).

[6] The local surface density (Σ) was computed with the 10 nearest neighbours to each galaxy belonging to the cluster.

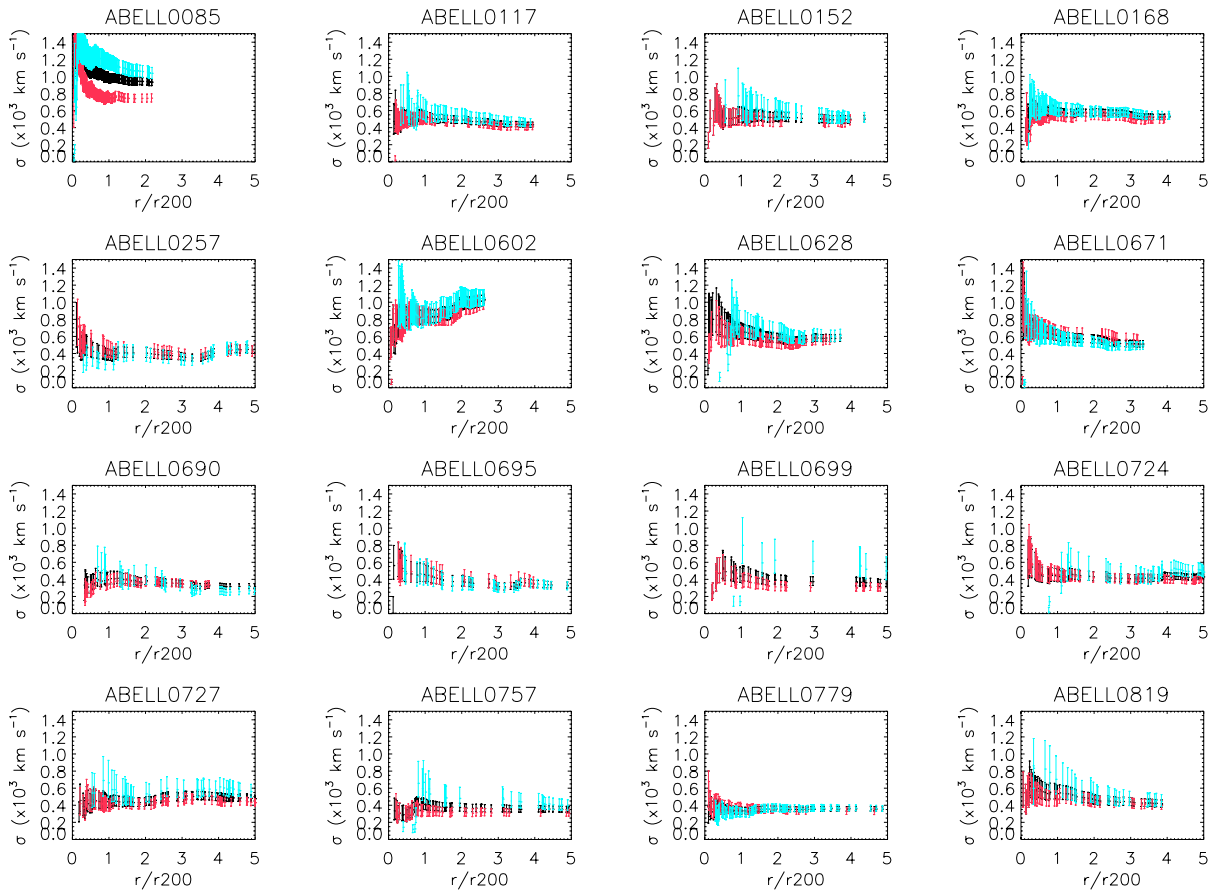

Fig. 6. Velocity dispersion profiles of some clusters of our sample. The black symbols represent the velocity dispersion profile taking all types of galaxies into account. Blue and red symbols represent the velocity dispersion profiles corresponding to blue and red galaxies.

of $\sigma_i/\sigma_{c,b}$ for the blue galaxies are: 1.15 ± 0.07, 1.04 ± 0.03, 0.95 ± 0.04, 0.93 ± 0.04, and 0.92 ± 0.04. In those computations, $\sigma_{c,r}$ and $\sigma_{c,b}$ represent the velocity dispersion of the red and blue galaxies within a radius equal to r_{200}, respectively. Figure 7 show, the distribution of $\sigma_i/\sigma_c, i = 1, 2, 3, 4, 5$ for the blue, red, and the total galaxy sample.

The VDPs have been studied in the literature by several authors. Most of them conclude that, for large radii ($r > 1$ Mpc), the VDPs are flat (Girardi & Mezzetti 2001; Rines & Diaferio 2006; Fadda et al. 1996; Muriel et al. 2002). This is consistent with the mild decrease that we have found in our clusters. The VDPs for red galaxies in our sample are almost flat outside r_{200}. This is not the case of the VDPs of blue galaxies, which clearly decrease with radius outside r_{200}. In the inner regions ($r < r_{200}$), the VDPs of the total sample and those corresponding to the red galaxies are flat. In contrast, the VDPs of blue galaxies decrease with radius. Different authors show that VDPs can decrease or increase with radius; e.g. den Hartog & Katgert (1996) made a thorough study and found that the variations of the VDPs in the innermost regions of clusters ($r < 0.5$ Mpc) are real and not due to noise or bad-centre election. We re-computed σ_1/σ_c and σ_2/σ_c only for those clusters with X-ray centres, and our results did not change significantly. Thus, we can conclude that, in our galaxy cluster sample, only blue galaxies show increasing VDPs towards the centre of the cluster, while red galaxies show flat VDPs.

The previous findings can also be seen in Fig. 8. We show the VDPs of the different galaxy classes for the normalised cluster, which was obtained by normalising the scales and velocities of each galaxy of the sample. Thus, the radial distance of each galaxy to the cluster centre was scaled by r_{200} of the corresponding cluster, and the relative velocity of each galaxy cluster was normalised by the velocity dispersion of the cluster. Figure 8 shows the VDPs that correspond to the total, bright ($M_r < M_r^* + 1$), and dwarf ($M_r > M_r^* + 1$) galaxy samples. We also distinguished between red and blue objects. The VDPs of the total galaxy sample indicate that blue galaxies always have larger velocity dispersion than red ones. They also show constantly decreasing VDPs, while red ones have almost constant and slowly decreasing VDPs inside and outside r_{200}, respectively. These features can also be seen in the VDPs of the bright galaxy sample. In contrast, red and blue dwarfs show decreasing VDPs inside r_{200}.

The shape of the VDPs can provide information about the dynamical state of the galaxies. Thus, clusters with galaxies predominantly in radial orbits produce an outwardly declining VDP. This is the case for the blue galaxies of our sample, which agrees with previous findings (Biviano & Katgert 2004; Adami et al. 1998). We also found that the red-dwarf galaxies inside r_{200} have an outwardly declining VDP. This would imply that this kind of galaxy may also be located in radial orbits. In contrast, constant VDPs imply an isotropic distribution of velocities (Solanes et al. 2001). This is the case for the red bright galaxy population inside r_{200}.

6. Fraction of blue galaxies

Butcher & Oemler (1984) observed that the fraction of blue galaxies (f_b) in clusters evolves with redshift, in the sense that

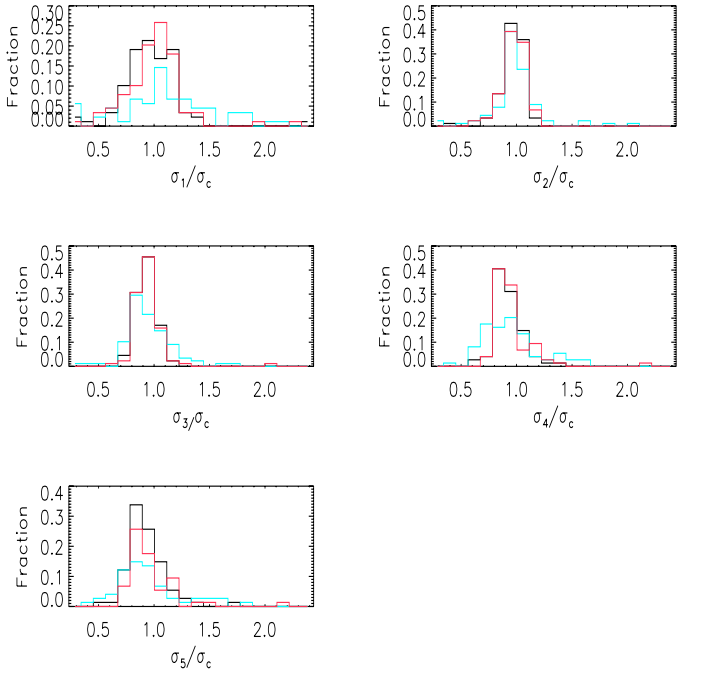

Fig. 7. Histograms of the ratios $\sigma_i/\sigma_c, i = 1, 2, 3, 4, 5$ for the galaxies in the clusters. The black full lines represent all galaxies,and the blue and red lines correspond to late- and early-type ones. See text for more details.

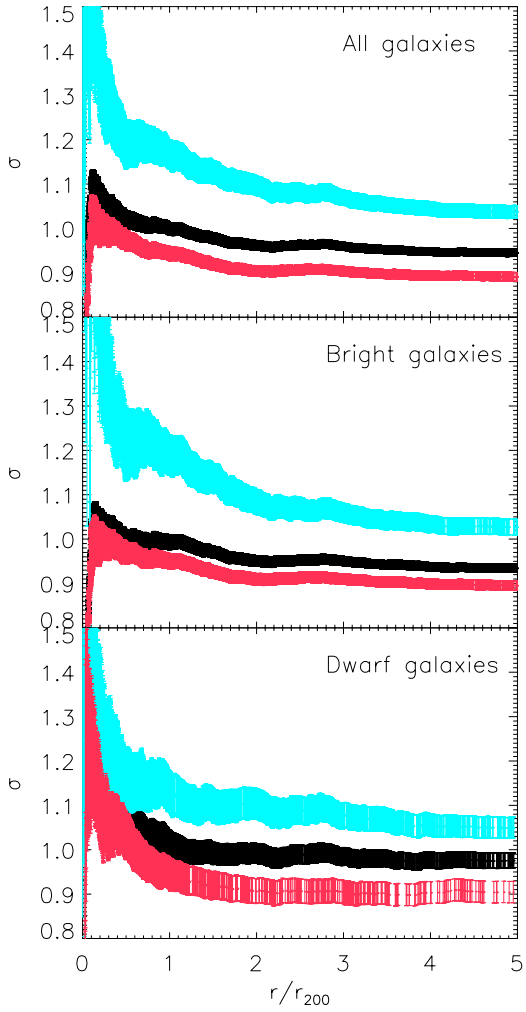

Fig. 8. Velocity dispersion profiles of the galaxies of the normalised cluster. The total galaxy population is shown in the top panel. Bright galaxies ($M_r < M_r^* + 1$) are in the middle panel, and the bottom panel shows the VDPs corresponding to the dwarf galaxy sample ($M_r > M_r^* + 1$). The VDP of the total, blue, and red galaxy samples are represented by black, blue, and red colours (see text for more details).

galaxy clusters located at medium redshift have a larger f_b than nearby ones. This has been usually interpreted as an evolutionary trend in clusters. But it is a matter of debate as to which is the role played by the environment in the change in the fraction of blue galaxies. We computed f_b in our sample of galaxy clusters, studying the variation with z and the possible influence of the environment.

6.1. Adopted aperture and limiting magnitude

The original analysis of Butcher & Oemler (1984) defined blue galaxies as those within a radius containing 30 percent of the cluster population, which are brighter than $M_v = -20$ and bluer by 0.2 mag in $B - V$ than the colour–magnitude relation defined by the cluster early-type galaxies. It has been noticed by several authors that the fraction of blue galaxies strongly depends on the magnitude limit and the clustercentric distance used (Ellingson et al. 2001; Goto et al. 2003; De Propris et al. 2004; Andreon et al. 2006). They observed that f_b grows when the magnitude limit is fainter and the aperture is larger, reflecting the existence of a large fraction of faint blue galaxies in the outer regions of the clusters. De Propris et al. (2004) considered if appropriate to measure f_b in apertures based on cluster physical properties. They used r_{200} as the aperture radius where they measured f_b for their clusters. We have also adopted this radius in order to determine f_b in our galaxy clusters. As previously commented, f_b also depends on the adopted limiting magnitude of the galaxies in clusters. It should be noticed that, as we move to higher redshifts, we systematically lose faint galaxies (see Fig. 2). Our clusters spread in a redshift range of $0.02 < z < 0.1$, and only galaxies brighter than $M_r = -20.0$ ($\approx M_r^* + 0.5$) can be observed at all redshifts. For this reason, we adopted this absolute magnitude as the limiting magnitude for the computation of f_b. This ensures we work with a complete galaxy sample at all redshifts. Other authors have adopted fainter limiting magnitudes, e.g. $M^* + 1.5$ (De Propris et al. 2004) or $M^* + 3$ (Margoniner & de Carvalho 2000). If there is a large number of blue galaxies at faint magnitudes, we expect that our values of f_b will be lower than those reported by the previous authors.

6.2. Colour–magnitude diagrams

We determined the $g - r$ versus r colour–magnitude diagrams for all the clusters in our sample. The colour–magnitude relation was measured by a robust fitting routine by minimising the absolute deviation in $g - r$ colour, using only early-type galaxies located within an aperture of radius equal to r_{200}. The galaxy types were determined according to the $u - r$ colour and the light galaxy concentration parameter, C_{in}. These two criteria allow us to identify the most reliable sample of E/S0 galaxies (see Shimasaku et al. 2001; Strateva et al. 2001). Thus, we considered early-type galaxies to be those with $u - r \geq 2.22$ and $C_{in} < 0.4$. Figure 9 shows the colour–magnitude diagrams of four representative galaxy clusters. The colour–magnitude relation fitted in each case is also overploted. Figure 9 (left column) also shows

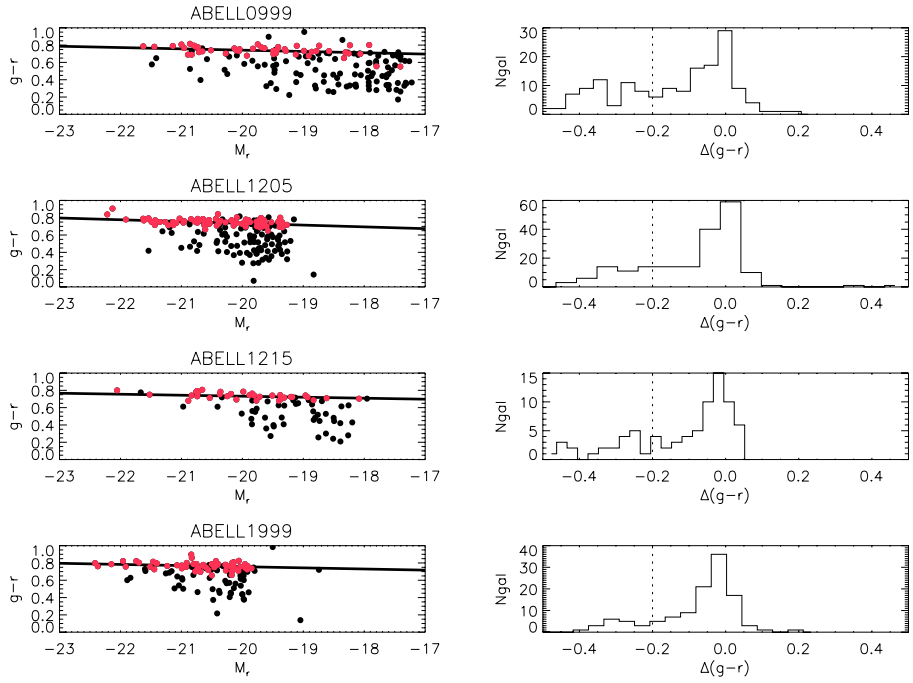

Fig. 9. Colour–magnitude relation (*left*) and histograms (*right*) of the marginalised colour distribution for four representative clusters at different redshifts of our cluster sample. The full line in left panels represent the fitted colour–magnitude relation. The vertical point lines in right panel represent the blue/red separation in the Butcher-Oemler effect. The red points are the galaxies with $u - r \geq 2.22$ and $C_{\rm in} < 0.4$ (see text for more details).

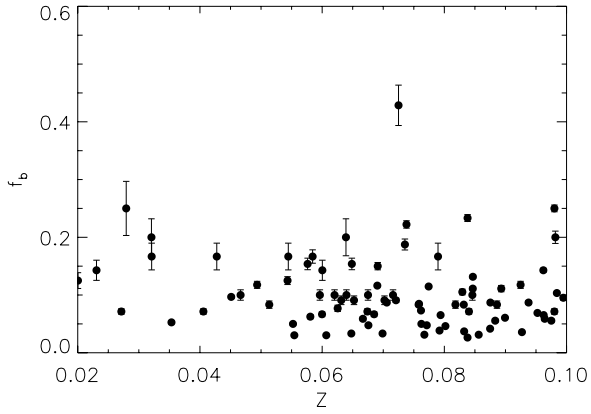

Fig. 10. The fraction of blue galaxies ($f_{\rm b}$) as a function of redshift of the galaxy clusters.

the histograms of the colour distribution, marginalised over the fitted colour–magnitude relation.

The average of the slopes of the colour–magnitude relations of the early-type galaxies of the clusters is -0.014 ± 0.008. This slope is within the errors, in agreement with the slope obtained by Gallazzi et al. (2006) for a large sample of galaxies using SDSS data. It also agrees with the average $B - R$ slope obtained by De Propris et al. (2004) for a sample of galaxy clusters from 2dFGRS.

6.3. Calculation the blue fraction of galaxies

As we explained before, the blue fraction of galaxies was computed using only those galaxies brighter than $M_r = -20$ and located within an aperture of radius r_{200}. In the present study we only used spectroscopically-confirmed galaxy-cluster members. This should not bias our results, especially due to our high completeness. Figure 10 presents $f_{\rm b}$ as a function of redshift. The errors of $f_{\rm b}$ were computed according to the prescription given by De Propris et al. (2004). We observed no evolution of $f_{\rm b}$ with redshift, which means that our sample is ideal to study the effects of the environment on $f_{\rm b}$.

We have considered three cluster properties (concentration, velocity dispersion and, X-ray luminosity) of each cluster in order to analyse the dependence of $f_{\rm b}$ on the environment. The concentration parameter was computed following the prescription of De Propris et al. (2004); i.e. $C = \log(r_{60}/r_{20})$, where r_{60} and r_{20} are the radii containing 60 and 20 percent of the cluster galaxies, respectively. The velocity dispersion of the clusters was taken from Table 1. The X-ray luminosities were obtained from the literature (Ebeling et al. 1998; Böhringer et al. 2000; Ebeling et al. 2000; and Ledlow et al. 2003), which were measured in the ROSAT band (0.1–2.4 keV). We only found X-ray data for 48 clusters of the sample.

Figure 11 shows the dependence of the fraction of blue galaxies on concentration, cluster velocity dispersion and, X-ray luminosity. The non-parametric Spearman test means that $f_{\rm b}$ has a low correlation with concentration and velocity dispersion. The fraction of blue galaxies correlates best with the velocity dispersion, but the significance of the correlation is 2.6σ. In contrast, the Spearman test shows a correlation between $f_{\rm b}$ and X-ray luminosity, where the significance of this correlation is just 3σ. Notice that the points are distributed in the $L_{\rm X} - f_{\rm b}$ plane following a triangular shape. Clusters with high X-ray luminosity ($L_{\rm X}(0.1{-}2.4\ {\rm keV}) > 10^{45}\ {\rm erg\,s^{-1}}$) show small fractions of blue galaxies (less than 10%). Nevertheless, those clusters with low X-ray luminosity show small and large fractions of blue galaxies. This correlation could indicate that there is a threshold over which cluster environment can affect the galaxy colours and play a role in the galaxy evolution. This means that, according to our $L_{\rm X} - \sigma$ relation, the evolution of galaxies could be driven by the cluster environment for those clusters with a velocity dispersion larger than $\sigma \approx 800\ {\rm km\,s^{-1}}$. Recently, Popesso et al. (2006) have found a similar correlation between $L_{\rm X}$ and $f_{\rm b}$ for a larger cluster sample. The shape of the our $L_{\rm X} - f_{\rm b}$ correlation is similar to the correlation between cluster velocity dispersion and the fraction of [OII] emitters for clusters at low redshift reported by Poggianti et al. (2006). They find that clusters with $\sigma > 550\ {\rm km\,s^{-1}}$ have a constant low fraction (less than 30%) of

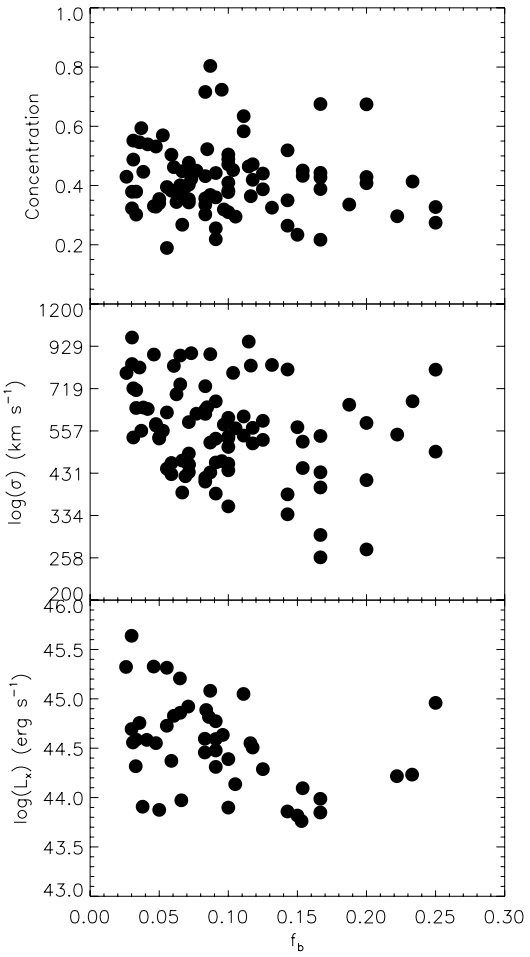

Fig. 11. The fraction of blue galaxies (f_b) as a function of galaxy distribution (*top*), cluster velocity dispersion (*middle*), and X-ray luminosity (*bottom*) of the galaxy clusters.

[OII] emitters. In contrast, those clusters with smaller σ show large and small fractions of [OII] emitters.

We recomputed f_b taking into account those galaxies within an aperture of radius equal to r_{200} and brighter than $M_r = -19.5$. We restricted the analysis only to those clusters with $z < 0.05$, because our sample is complete down to $M_r = -19.5$ in this redshift range. In this case the number of cluster decreases to 13. We have again studied the correlations of f_b with galaxy concentration, velocity dispersion, and X-ray luminosity, obtaining similar correlations to the full sample.

7. Discussion

From the study presented in this paper, most of the galaxies (62%) located in the central regions of galaxy clusters ($r/r_{200} < 2$) are early-type galaxies (see Sect. 4). In contrast, the field population is dominated by late-type galaxies. In the literature it is also well-established that the colour of galaxies in clusters and the field is different, an indication of the low star-formation activity found in cluster galaxies (e.g. Balogh et al. 1998; Lewis et al. 2002; Gómez et al. 2003). These differences in morphology and stellar content between field and cluster galaxies suggest different evolutionary processes. That late-type galaxies show larger velocity dispersions and are located at larger distances from the cluster centre than early-type ones has been interpreted as late-type galaxies being recent arrivals to the cluster potential, forming a non-relaxed group of galaxies moving in more radial orbits than early-type ones (e.g. Stein 1997; Adami et al. 1998). As late-type galaxies fall into the cluster potential and encounter denser environments, they evolve to early-type ones. The results presented in the present work agrees with previous findings. However, as pointed out by Goto (2005), this would imply that a large fraction of galaxies (≈40% according to our sample) should be recent arrivals to the cluster, a possibility that seems unlikely. Goto (2005) conclude that the different observational properties between red and blue galaxies may indicate which is the main mechanism driving the evolution of galaxies in clusters. Gas stripping, mergers, and interactions with other galaxies and with the cluster potential are the main mechanisms able to transform galaxies in clusters, making late-type galaxies lose their gas content, stop their star formation, circularise their orbits, and transform their morphology from disk-like objects to spheroids. All of these mechanisms affect galaxies in clusters, but can we infer from the observational results which the dominant one is?.

It should be noted that the different mechanisms of galaxy evolution have very different timescales. While gas stripping has a very short timescale (≈50 Myr, Quilis et al. 2000), the galaxy infall process can take ≈1 Gyr. The different mechanisms also have different underlying physics. Thus, ram-pressure stripping is proportional to the density of the intracluster medium (ICM) and to the square of the velocity of the galaxy. In contrast, dynamical interactions are more efficient when the relative velocity of galaxies is lower (Mamon 1992). This means that gas stripping is stronger in the cluster centres and for galaxies with high velocities, while dynamical interactions should be more efficient for galaxies with smaller velocity dispersions. Numerical simulations have shown that most of the galaxies inside the virial radius have already been through the cluster core more than once (Mamon et al. 2004). If gas stripping were the main mechanism driving galaxy evolution in clusters, according to the short time scale of this process, only a few blue (late-type) galaxies should be observed in the central regions of clusters. Moreover, gas stripping is also stronger in galaxies with larger velocity dispersion, which means that late-type galaxies should be more affected by this mechanism than early-type ones.

Based on these considerations, Goto (2005) have concluded that gas stripping is not the main responsible mechanism driving the evolution of galaxies in clusters. Instead, galaxies in clusters evolve mainly by dynamical interactions. We can add to Goto's discussion that if gas stripping were the main galactic evolution mechanism in clusters, then the fraction of blue galaxies should depend on the cluster mass as the temperature and density of the gas increases with the cluster mass. According to our results, this is true for those clusters with high X-ray luminosities. In contrast, the cluster environment is not so important in driving the evolution of galaxies in low-mass clusters. Thus, gas stripping may not be the main mechanism responsible for transforming late-type to early-type galaxies in low-mass clusters, but could be important in the most massive ones. This does not mean that gas stripping is absent in the evolution of galaxies in clusters; some clear examples of gas stripping have been observed in galaxies in Virgo (Kenney et al. 2004).

Dynamical interactions include interactions both with the cluster potential and with other galaxies. These effects can trigger temporary star formation in cluster galaxies (Fujita 1998), which can be analysed by studying their colour distribution. These interactions can also disrupt stars from galaxies, forming at the beginning long tidal tails that subsequently will be diluted and will form the diffuse light observed in some nearby clusters

like Virgo (see Aguerri et al. 2005b, and references therein). These effects will be greater in those galaxies with lower relative velocities. Fujita (1998) concludes that, if the tidal effects enhance the SFR in the galaxies, then the bluest galaxies should be located close to the cluster centre (within ≈300 kpc), whereas they should be in the outer parts of the cluster if the SFR is induced by galaxy-galaxy encounters. We have investigated the fraction of blue galaxies in our clusters located within 300 kpc of the centre of the cluster. The sample has been divided into bright and dwarf galaxies ($M_r < M_r^*+1$ and $M_r > M_r^*+1$, respectively). We found that 40% of the blue bright galaxies and 30% of the blue dwarf ones are located at smaller distance than 300 kpc from the cluster centre. This means that tidal interactions with the cluster potential are not the responsible mechanism for the formation of most of the blue galaxies in our clusters. The lack of blue galaxies in the central regions of clusters has also been observed in nearby clusters like Coma (Aguerri et al. 2004), as well as in other distant clusters (Rakos et al. 1997; Abraham et al. 1996; Balogh et al. 1997).

These pieces of evidence indicate that the evolution of galaxies in clusters could be driven by the cluster environment in the most massive ones, but galaxies in low-mass clusters could evolve mainly due to the local environment.

8. Conclusions

In the present paper we have analysed the main properties of the galaxies of one of the largest (10865 galaxies) and homogeneous samples ever presented in the literature. The galaxies were grouped into two families according to their $u-r$ colour. Those galaxies with $u-r \geq 2.22$ formed the red (early-type) family and those with $u-r < 2.22$ the blue (late-type) one. We derived the position, velocity dispersion, and VDPs of both families of galaxies, obtaining:

- Within $2\times r_{200}$, 62% and 38% of the galaxies turned outto be red and blue, respectively.
- The median positions and velocity dispersions are lower for red galaxies than for blue ones.
- Bright ($M_r < M_r^* - 1$) and dwarf ($M_r > M_r^* + 1$) red galaxies are located at shorter distances than the blue ones, sharing the same cluster environment.
- The brightest cluster members ($M_r < -21.0$) show smaller velocity dispersions than the rest of them.
- The VDPs of the total galaxy cluster population are constant with radius in the central regions of the clusters ($r < r_{200}$), while slowly decreasing in the outermost regions ($r \geq r_{200}$). The red galaxy population also has flat VDPs in the central regions ($r < r_{200}$). In contrast, the VDPs of blue galaxies grow towards the cluster centre. In the outer regions ($r > r_{200}$), the VDPs of red galaxies decline smoothly with radius, while the decrement is faster for blue ones. This indicates that the galaxies in the outermost regions of the clusters are dominated by the blue population and have more radial and anisotropic orbits than galaxies in the inner regions dominated by the red population.
- The fraction of blue galaxies in our cluster sample does not correlate with cluster global properties, such as the concentration of the galaxy distribution and cluster velocity dispersion. However, we find a correlation between the X-ray luminosity and the fraction of blue galaxies. Those clusters with $L_X(0.1-2.4\,\mathrm{keV}) > 10^{45}\,\mathrm{erg\,s^{-1}}$ have a low fraction of blue galaxies (less than 10%). In contrast, clusters with low X-ray luminosity show both large and small fractions of blue galaxies. This could indicate that the star formation in cluster galaxies may be regulated by global cluster properties for clusters with $L_X(0.1-2.4\,\mathrm{keV}) > 10^{45}\,\mathrm{erg\,s^{-1}}$, i.e. those clusters with $\sigma_c > 800\,\mathrm{km\,s^{-1}}$.

All these results agrees with previous findings from other cluster samples, indicating that red and blue galaxies have different evolutions in galaxy clusters. We have discussed these results according to the different galaxy transformation mechanisms presented in galaxy clusters, concluding that the local environment plays a key role in galaxy evolution in low-mass clusters, while the evolution of galaxies in massive clusters could be driven by the global cluster environment.

Acknowledgements. We wish to thank the anonymous referee for useful coments that have improved this manuscript. We acknowledge financial support by the Spanish Ministerio de Ciencia y Tecnología grants AYA2004-08260. We would also like to thank T. Beers for providing us with a copy of his code ROSTAT, and K. M. Ashman and S. Zepf for making their KMM code available to us. Funding for the SDSS and SDSS-II has been provided by the Alfred P. Sloan Foundation, the Participating Institutions, the National Science Foundation, the U.S. Department of Energy, the National Aeronautics and Space Administration, the Japanese Monbukagakusho, the Max Planck Society, and the Higher Education Funding Council for England. The SDSS Web Site is `http://www.sdss.org/`. The SDSS is managed by the Astrophysical Research Consortium for the Participating Institutions. The Participating Institutions are the American Museum of Natural History, Astrophysical Institute Potsdam, University of Basel, Cambridge University, Case Western Reserve University, University of Chicago, Drexel University, Fermilab, the Institute for Advanced Study, the Japan Participation Group, Johns Hopkins University, the Joint Institute for Nuclear Astrophysics, the Kavli Institute for Particle Astrophysics and Cosmology, the Korean Scientist Group, the Chinese Academy of Sciences (LAMOST), Los Alamos National Laboratory, the Max-Planck-Institute for Astronomy (MPIA), the Max-Planck-Institute for Astrophysics (MPA), New Mexico State University, Ohio State University, University of Pittsburgh, University of Portsmouth, Princeton University, the United States Naval Observatory, and the University of Washington. This research has made use of the NASA/IPAC Extragalactic Database (NED) which is operated by the Jet Propulsion Laboratory, California Institute of Technology, under contract with the National Aeronautics and Space Administration.

References

Abell, G. O., Corwin, H. G., Jr., & Olowin, R. P. 1989, ApJS, 70, 1
Abraham, R. G., Smecker-Hane, T. A., Hutchings, J. B., et al. 1996, ApJ, 471, 694
Adami, C., Biviano, A., & Mazure, A. 1998, A&A, 331, 439
Adelman-McCarthy, J. K., Agüeros, M. A., Allam, S. S., et al. 2006, ApJS, 162, 38
Aguerri, J. A. L., Iglesias-Paramo, J., Vilchez, J. M., & Muñoz-Tuñón, C. 2004, AJ, 127, 1344
Aguerri, J. A. L., Iglesias-Páramo, J., Vílchez, J. M., Muñoz-Tuñón, C., & Sánchez-Janssen, R. 2005a, AJ, 130, 475
Aguerri, J. A. L., Gerhard, O. E., Arnaboldi, M., et al. 2005b, AJ, 129, 2585
Aguerri, J. A. L., Castro-Rodríguez, N., et al. 2006, A&A, 457, 771
Akritas, M. G., & Bershady, M. A. 1996, ApJ, 470, 706
Andreon, S., & Ettori, S. 1999, ApJ, 516, 647
Andreon, S., Davoust, E., Michard, R., Nieto, J.-L., & Poulain, P. 1996, A&AS, 116, 429
Andreon, S., Quintana, H., Tajer, M., Galaz, G., & Surdej, J. 2006, MNRAS, 365, 915
Arnaboldi, M., Aguerri, J. A. L., Napolitano, N. R., et al. 2002, AJ, 123, 760
Arnaboldi, M., Gerhard, O., Aguerri, J. A. L., et al. 2004, ApJ, 614, L33
Ashman, K. M., Bird, C. M., & Zepf, S. E. 1994, AJ, 108, 2348
Balogh, M. L., Morris, S. L., Yee, H. K. C., Carlberg, R. G., & Ellingson, E. 1997, ApJ, 488, L75
Balogh, M. L., Schade, D., Morris, S. L., et al. 1998, ApJ, 504, L75
Beers, T. C., Flynn, K., & Gebhardt, K. 1990, AJ, 100, 32
Bekki, K., Couch, W. J., & Shioya, Y. 2002, ApJ, 577, 651
Biviano, A., & Girardi, M. 2003, ApJ, 585, 205
Biviano, A., & Katgert, P. 2004, A&A, 424, 779
Biviano, A., Girardi, M., Giuricin, G., Mardirossian, F., & Mezzetti, M. 1992, ApJ, 396, 35
Blanton, M. R., Brinkmann, J., Csabai, I., et al. 2003, AJ, 125, 2348
Blanton, M. R., Lupton, R. H., Schlegel, D. J., et al. 2005, ApJ, 631, 208

Böhringer, H., Voges, W., Huchra, J. P., et al. 2000, ApJS, 129, 435
Borgani, S., Girardi, M., Carlberg, R. G., Yee, H. K. C., & Ellingson, E. 1999, ApJ, 527, 561
Butcher, H., & Oemler, A. 1984, ApJ, 285, 426
Carlberg, R. G., Yee, H. K. C., & Ellingson, E. 1997, ApJ, 478, 462
Castro-Rodríguez, N., Aguerri, J. A. L., Arnaboldi, M., Gerhard, O., Freeman, K. C., Napolitano, N. R., & Capaccioli, M. 2003, A&A, 405, 803
Cole, S., & Lacey, C. 1996, MNRAS, 281, 716
Colless, M., Dalton, G., Maddox, S., et al. 2001, MNRAS, 328, 1039
Curtis, H. D. 1918, Publications of Lick Observatory, 13, 55
Danese, L., de Zotti, G., & di Tullio, G. 1980, A&A, 82, 322
den Hartog, R., & Katgert, P. 1996, MNRAS, 279, 349
De Propris, R., Colless, M., Driver, S. P., et al. 2003, MNRAS, 342, 725
De Propris, R., Colless, M., Peacock, J. A., et al. 2004, MNRAS, 351, 125
Dressler, A. 1980, ApJ, 236, 351
Dressler, A., Oemler, A. Jr., Couch, W. J., et al. 1997, ApJ, 490, 577
Ebeling, H., Edge, A. C., Bohringer, H., Allen, S. W., Crawford, C. S., Fabian, A. C., Voges, W., & Huchra, J. P. 1998, MNRAS, 301, 881
Ebeling, H., Edge, A. C., Allen, S. W., Crawford, C. S., Fabian, A. C., & Huchra, J. P. 2000, MNRAS, 318, 333
Edge, A. C., & Stewart, G. C. 1991, MNRAS, 252, 414
Ellingson, E., Lin, H., Yee, H. K. C., & Carlberg, R. G. 2001, ApJ, 547, 609
Fadda, D., Girardi, M., Giuricin, G., Mardirossian, F., & Mezzetti, M. 1996, ApJ, 473, 670
Fairley, B. W., Jones, L. R., Wake, D. A., et al. 2002, MNRAS, 330, 755
Fasano, G., Poggianti, B. M., Couch, W. J., et al. 2000, ApJ, 542, 673
Fujita, Y. 1998, ApJ, 509, 587
Gallazzi, A., Charlot, S., Brinchmann, J., & White, S. D. M. 2006, MNRAS, 370, 1106
Girardi, M., & Mezzetti, M. 2001, ApJ, 548, 79
Girardi, M., Fadda, D., Giuricin, G., Mardirossian, F., Mezzetti, M., & Biviano, A. 1996, ApJ, 457, 61
Gómez, P. L., Nichol, R. C., Miller, C. J., et al. 2003, ApJ, 584, 210
Goto, T. 2005, MNRAS, 359, 1415
Goto, T., Okamura, S., Yagi, M., et al. 2003, PASJ, 55, 739
Gott, J. R. I. 1972, ApJ, 173, 227
Gunn, J. E., & Gott, J. R. I. 1972, ApJ, 176, 1
Gutiérrez, C. M., Trujillo, I., Aguerri, J. A. L., Graham, A. W., & Caon, N. 2004, ApJ, 602, 664
Haines, C. P., La Barbera, F., Mercurio, A., Merluzzi, P., & Busarello, G. 2006, ApJ, 647, L21
Hilton, M., et al. 2005, MNRAS, 363, 661
Hogg, D. W., Finkbeiner, D. P., Schlegel, D. J., & Gunn, J. E. 2001, AJ, 122, 2129
Hogg, D. W., Blanton, M. R., Brinchmann, J., et al. 2004, ApJ, 601, L29
Hubble, E., & Humason, M. L. 1931, ApJ, 74, 43
Katgert, P., Mazure, A., den Hartog, R., Adami, C., Biviano, A., & Perea, J. 1998, A&AS, 129, 399
Katgert, P., Biviano, A., & Mazure, A. 2004, ApJ, 600, 657
Kenney, J. D. P., van Gorkom, J. H., & Vollmer, B. 2004, AJ, 127, 3361
Ledlow, M. J., Voges, W., Owen, F. N., & Burns, J. O. 2003, AJ, 126, 2740
Lewis, I., Balogh, M., De Propris, R., et al. 2002, MNRAS, 334, 673
Lupton, R. H., Ivezic, Z., Gunn, J. E., Knapp, G., Strauss, M. A., & Yasuda, N. 2002, Proc. SPIE, 4836, 350
Mahdavi, A., & Geller, M. J. 2001, ApJ, 554, L129
Mamon, G. A. 1992, ApJ, 401, L3
Mamon, G. A., Sanchis, T., Salvador-Solé, E., & Solanes, J. M. 2004, A&A, 414, 445
Mastropietro, C., Moore, B., Mayer, L., Debattista, V. P., Piffaretti, R., & Stadel, J. 2005, MNRAS, 364, 607
Margoniner, V. E., & de Carvalho, R. R. 2000, AJ, 119, 1562
Margoniner, V. E., de Carvalho, R. R., Gal, R. R., & Djorgovski, S. G. 2001, ApJ, 548, L143
Melnick, J., & Sargent, W. L. W. 1977, ApJ, 215, 401
Metevier, A. J., Romer, A. K., & Ulmer, M. P. 2000, AJ, 119, 1090
Miller, C. J., Nichol, R. C., Reichart, D., et al. 2005, AJ, 130, 968
Moore, B., Katz, N., Lake, G., Dressler, A., & Oemler, A. 1996, Nature, 379, 613
Moss, C., & Dickens, R. J. 1977, MNRAS, 178, 701
Mulchaey, J. S., & Zabludoff, A. I. 1998, ApJ, 496, 73
Muriel, H., Quintana, H., Infante, L., Lambas, D. G., & Way, M. J. 2002, AJ, 124, 1934
Oemler, A. J. 1974, ApJ, 194, 1
Ortiz-Gil, A., Guzzo, L., Schuecker, P., Böhringer, H., & Collins, C. A. 2004, MNRAS, 348, 325
Pier, J. R., Munn, J. A., Hindsley, R. B., et al. 2003, AJ, 125, 1559
Pisani, A. 1993, MNRAS, 278, 697
Poggianti, B. M., von der Linden, A., De Lucia, G., et al. 2006, ApJ, 642, 188
Popesso, P., Biviano, A., Bohringer, H., & Romaniello, M. 2006 [arXiv:astro-ph/0606191]
Quilis, V., Moore, B., & Bower, R. 2000, Science, 288, 1617
Quintana, H., & Melnick, J. 1982, AJ, 87, 972
Rakos, K. D., Odell, A. P., & Schombert, J. M. 1997, ApJ, 490, 194
Rines, K., & Diaferio, A. 2006, AJ, 132, 1275
Rines, K., Geller, M. J., Kurtz, M. J., & Diaferio, A. 2003, AJ, 126, 2152
Schlegel, D. J., Finkbeiner, D. P., & Davis, M. 1998, ApJ, 500, 525
Shimasaku, K., Fukugita, M., Doi, M., et al. 2001, AJ, 122, 1238
Smail, I., Edge, A. C., Ellis, R. S., & Blandford, R. D. 1998, MNRAS, 293, 124
Sodre, L. J., Capelato, H. V., Steiner, J. E., & Mazure, A. 1989, AJ, 97, 1279
Solanes, J. M., Manrique, A., García-Gómez, C., González-Casado, G., Giovanelli, R., & Haynes, M. P. 2001, ApJ, 548, 97
Stein, P. 1997, A&A, 317, 670
Strateva, I., Ivezić, Ž., Knapp, G. R., et al. 2001, AJ, 122, 1861
Strauss, M. A., Weinberg, D. H., Lupton, R. H., et al. 2002, AJ, 124, 1810
Tammann, G. A. 1972, A&A, 21, 355
Xue, Y.-J., & Wu, X.-P. 2000, ApJ, 538, 65
Voges, W., Aschenbach, B., Boller, Th., et al. 1999, A&A, 349, 389
Yahil, A., & Vidal, N. V. 1977, ApJ, 214, 347
York, D. G., Adelman, J., Anderson, J. E. Jr., et al. 2000, AJ, 120, 1579
Zabludoff, A. I., Huchra, J. P., & Geller, M. J. 1990, ApJS, 74, 1
Zwicky, F., Herzog, E., & Wild, P. 1961, Pasadena: California Institute of Technology (CIT)